Iraqi Journal of Physics, 2019 *Vol.17, No.42, PP. 1-12*

DOI: 10.20723/ijp.17.42.1-12

Study of ground state properties of some Ni-Isotopes using Skyrme-Hartree-Fock method

Ehsan M. Raheem, Ali A. Abdul Hasan, Imad H. Alwan

Directorate of Nuclear Researches and Applications, Ministry of Science and Technology, Baghdad, Iraq

E-mail: ehsan.nucl@yahoo.com

Abstract

The nuclear ground-state properties of some Nickel ($^{58-66}$Ni) isotopes have been investigated within the framework of the mean field approach using the self-consist Hartree-Fock calculations (HF) including the effective interactions of Skyrme. The Skyrme parameterizations SKM, SKM*, SI, SIII, SKO, SKE, SLY4, SKxs15, SKxs20 and SKxs25 have been utilized with HF method to study the nuclear ground state charge, mass, neutron and proton densities with the corresponding root mean square radii, charge form factors, binding energies and neutron skin thickness. The deduced results led to specifying one set or more of Skyrme parameterizations that used to achieve the best agreement with the available experimental data.

Key words

Nuclear ground-state properties, Skyrme interaction, Skyrme-Hartree-Fock method, nuclear density, Nickel isotopes.

Article info.

Received: Feb. 2019
Accepted: Apr. 2019
Published: Sep. 2019

دراسة خصائص الحالة الأرضية لبعض نظائر النيكل باستخدام طريقة سكيرم – هارتري – فوك

احسان مشعان رحيم، علي احمد عبدالحسن، عماد حسين علوان

مديرية البحوث و التطبيقات النووية، وزارة العلوم و التكنولوجيا، بغداد، العراق

الخلاصة

تمت دراسة خصائص الحالة الأرضية لبعض نظائر النيكل ($^{58-66}$Ni) باستخدام حسابات هارتري-فوك المتضمنة تفاعلات سكيرم المؤثرة. تم استخدام العديد من بارامترات سكيرم وهي SKM, SKM*, SI, SIII, SKO, SKE, SLY4, SKxs15, SKxs20, SKxs25 في حسابات كثافة الشحنة والكتلة والنيوترون والبروتون في الحالة الأرضية للنواة وانصاف الأقطار المرافقة لها أضافة الى عوامل تشكل الشحنة وطاقات الربط النووية والسمك النيوتروني. ان النتائج التي تم الحصول عليها أدت الى تحديد واحد أو أكثر من بارامترات سكيرم يحقق أفضل توافق مع النتائج العملية التي تمت المقارنة معها.

Introduction

The detailed theoretical concepts and studies that concern the nuclear structure of the stable nuclei and the nuclei that located near the stability valley require comprehensive microscopic theoretical studies and feasible calculations. For this purpose, self-consistent mean-field methods, such as Hartree-Fock (HF) method with effective interactions were applied successfully. The forms and parameters of the nucleon-nucleon forces were constructed by comparing the calculated nuclear radii and binding energies with experimental results. Skyrme interaction [1] is considered as a most common effective interaction

that leads to a considerable simplification of HF calculations.

Hartree-Fock method linked with Skyrme interaction (SHF) construct an efficacious model that has the significant effect to explain various nuclear properties such as density distributions, nuclear radii and deformations [2,3]. These quantities offer the precise test for many nuclear models and provide the valuable details concerning the structure of nuclei.

The nuclear charge density distribution (CDD) is considered as a ground state feature that studied extensively, accessible easily by the experiments of electron scattering, and provides the important data about the spatial distributions of the nuclear charge. The charge form factor is simply related to the charge density, and hence the both observables carry exactly the same amount of information [4].

The nuclear ground state properties are studied extensively with using SKM*, SKM and SLY4 Skyrme forces where SKM* force parameters were developed as a form of SKM [5].

Several researches [6-11] adopted the SHF method with different parameterizations to study the ground state nuclear structure of stable and unstable nuclei such as the nuclear density distributions, nuclear radii and nuclear binding energies.

In the present research, some static ground state properties of $^{58-66}$Ni isotopes have been investigated by using SHF method with Skyrme set parameters: SKM [12], SKM* [12], SI [2], SIII [13], SKO [14], SKE [15], SLY4 [16], SKxs15 [17], SKxs20 [17] and SKxs25 [17]. The obtained results have been compared with the available experimental data.

Theoretical framework

The Skyrme effective interaction is considered as a most convenient force used in addition to HF calculations to describe the nuclear ground state properties. This force consists of the momentum dependent two-body term $v_{ij}^{(2)}$ and the zero-range three-body term $v_{ijk}^{(3)}$ [1, 2, 18]:

$$\hat{V}_{Skyrme} = \sum_{i<j} v_{ij}^{(2)} + \sum_{i<j<k} v_{ijk}^{(3)} + t_2\hat{k}'^2\delta_{ij}\hat{k} + it_4\left(\hat{\sigma}_i - \hat{\sigma}_j\right).\hat{k}' \times \delta_{ij}\hat{k} \quad (1)$$

with:

$$v_{ij}^{(2)} = t_0(1 + x_0P_\sigma)\delta_{ij} + \frac{1}{2}t_1\left[\delta_{ij}\hat{k}'^2 + \hat{k}'^2\delta_{ij}\right] \quad (2)$$

$$v_{ijk}^{(3)} = t_3\,\delta_{ij}\,\delta_{jk} \quad (3)$$

For even-even spin saturated nuclei, we have:

$$v_{ijk}^{(3)} \approx v_{ij}^{(2)} = \frac{1}{6}\,t_3(1 + P_\sigma)\rho_0^\alpha(R)\,\delta_{ij} \quad (4)$$

with:

$$\hat{P}_\sigma = \frac{1}{2}\left(1 + \hat{\sigma}_i.\hat{\sigma}_j\right) \quad (5)$$

where $\boldsymbol{\delta_{ij}} = (\boldsymbol{r_i} - \boldsymbol{r_j})$, $\boldsymbol{\delta_{jk}} = (\boldsymbol{r_j} - \boldsymbol{r_k})$ are the delta functions, $\boldsymbol{\sigma}$ is the Pauli spin matrices $\boldsymbol{P_\sigma}$ is spin-exchange operator and $\boldsymbol{\rho_0(R)}$ is the isoscalar density. The vectors $\boldsymbol{k}$ and $\boldsymbol{k'}$ are the relative (momentum) wave vectors operators of two nucleons acting to the right and to the left, respectively; and given by:

$$\hat{k} = \frac{1}{2i}\left(\vec{\nabla}_i - \vec{\nabla}_j\right) \ , \ \hat{k}' = -\frac{1}{2i}\left(\vec{\nabla}_i - \vec{\nabla}_j\right) \quad (6)$$

The density dependent Skyrme interaction has the form [19]:

$$\hat{V}_{Skyrme}(R,r) = t_0\left(1 + x_0\hat{P}_\sigma\right)\delta(r) + \frac{1}{6}t_3\left(1 + x_3\hat{P}_\sigma\right)\rho_0^\alpha(R)\delta(r) + \frac{1}{2}t_1\left(1 + x_1\hat{P}_\sigma\right)\left[\hat{k}'^2\delta(r) + \delta(r)\hat{k}^2\right] + t_2\left(1 + x_2\hat{P}_\sigma\right)\hat{k}'.\delta(r)\hat{k} + iW_0\left(\hat{\sigma}_i + \hat{\sigma}_j\right).\hat{k}' \times \delta(r)\hat{k} \quad (7)$$

where $R = (r_i + r_j)/2$ and $r = r_i - r_j$ are the center of mass coordinates and the relative distance, respectively. $t_0, t_1, t_2, t_3, W_0, x_0, x_1, x_2, x_3$ and α are the Skyrme free parameters describing the strengths of different interaction terms. These parameters are determined from the comparison between the calculated and the experimental nuclear ground state properties such as binding energies, nucleon densities and root mean square radii.

In the SHF method, the total binding energy is expressed by the sum of kinetic, Skyrme, Coulomb, pairing energies in addition to the correction of the spurious motion [20].

$$E = \varepsilon_{kin} + \int d^3r \ \varepsilon_{Sky} + \varepsilon_{Coul} + \varepsilon_{Pair} - \varepsilon_{cm} \quad (8)$$

The kinetic energy of the nucleons is given by [21]:

$$\varepsilon_{kin} = \int d^3r \left(\frac{\hbar^2}{2\,m_P}\tau_P + \frac{\hbar^2}{2\,m_n}\tau_n\right) \quad (9)$$

where τ_n and τ_P are the kinetic energy densities of neutrons and protons, respectively.

The Skyrme energy takes the form [22]:

$$\varepsilon_{Sky} = \tfrac{1}{2}t_0\left[\left(1 + \tfrac{1}{2}x_0\right)\rho^2 - \left(x_0 + \tfrac{1}{2}\right)(\rho_n^2 + \rho_P^2)\right] + \tfrac{1}{12}t_3\rho^\alpha\left[\left(1 + \tfrac{1}{2}x_3\right)\rho^2 - \left(x_3 + \tfrac{1}{2}\right)(\rho_n^2 + \rho_P^2)\right] + \tfrac{1}{4}\left[t_1\left(1 + \tfrac{1}{2}x_1\right) + t_2\left(1 + \tfrac{1}{2}x_2\right)\right]\tau_P + \tfrac{1}{4}\left[t_2\left(x_2 + \tfrac{1}{2}\right) - t_1\left(x_1 + \tfrac{1}{2}\right)\right](\tau_n\rho_n + \tau_P\rho_P)\tfrac{1}{16} .\left[3t_1\left(1 + \tfrac{1}{2}x_1\right) - t_2\left(1 + \tfrac{1}{2}x_2\right)\right](\nabla\rho)^2 - \tfrac{1}{16}\left[3t_1\left(x_1 + \tfrac{1}{2}\right) + t_2\left(x_2 + \tfrac{1}{2}\right)\right] . \ [(\nabla\rho_n)^2 + (\nabla\rho_P)^2] + \frac{1}{2}W_0[J.\nabla\rho + J_n.\nabla\rho_n + J_P.\nabla\rho_P] \quad (10)$$

with:

$\tau = \tau_n + \tau_P$ Kinetic energy densities
$\rho = \rho_n + \rho_P$ Local nucleon densities (11)
$J = J_n + J_P$ Spin-orbit densities

Coulomb part depends only on the charge density and assigned as a sum of the direct term and exchange term. The contribution of the exchange term is due to the fact that the Coulomb interaction is infinite range. The Coulomb energy is given by [23]:

$$\varepsilon_{Coul} = \varepsilon_{Coul}^{dir} + \varepsilon_{Coul}^{ex} \quad (12)$$

where the direct term is given by:

$$\varepsilon_{Coul}^{dir} = \frac{e^2}{2}\int\int \frac{\rho_P(r)\,\rho_P(r')}{|r - r'|}\,dr\,dr' \quad (13)$$

and the exchange term is given by:

$$\varepsilon_{Coul}^{ex} = -\frac{4}{3}\,e^2\left(\frac{3}{\pi}\right)^{1/3}\int \rho_P\,(r)^{4/3}\,dr \quad (14)$$

with $e^2 = 1.44$ MeV.fm

The pairing energy of the two-nucleon interaction is given by [21]:

$$\varepsilon_{Pair} = \frac{1}{4}\sum_{q\in\{P,n\}} V_{Pair,q}\int d^3r \ \chi_q^2\left[1 - \frac{\rho(r)}{\rho_{0,Pair}}\right] \quad (15)$$

with:

$$\chi_q^2 = \sum_{\alpha \in q} f_\alpha \, u_\alpha \, v_\alpha \, |\phi_\alpha|^2 \qquad (16)$$

The strength V_{Pair} is adjusted for each Skyrme parameterization. The term $\rho_{0,Pair}$ represents the nuclear saturation density that is typically equal to $\rho_{0,Pair}$= 0.16 fm^{-3}, while χ and ρ are the pairing and particle densities, respectively. ϕ_α is the single particle state, f_α is the phase-space weight, v_α and u_α are the occupation and non-occupation amplitudes, respectively; where $u_\alpha^2 + v_\alpha^2 = 1$. The center of mass energy is given by [13]:

$$\varepsilon_{cm} = \frac{\langle P_{cm}^2 \rangle}{2Am} \qquad (17)$$

with:

$$\langle P_{cm}^2 \rangle = \sum w_\beta \, \langle \varphi_\beta | P^2 | \varphi_\beta \rangle - \sum \left(w_\alpha w_\beta + \sqrt{w_\alpha (1 - w_\alpha) \, w_\beta (1 - w_\beta)} \right) \left| \langle \phi_\alpha | P^2 | \phi_\beta \rangle \right|^2 \qquad (18)$$

where $P_{cm} = \sum_i P_i$ is the total momentum operator of the center of mass, P is the momentum operator, m is the average nucleon mass, A is the nucleon number, w_α and w_β are the occupation probabilities of the states ϕ_α and ϕ_β, respectively.

The charge, neutron and proton densities in spherical representation are given by [14, 19]:

$$\rho_k(r) = \sum_{\beta \in k} w_\beta \; \phi_\beta(r)^* \, \phi_\beta(r) \; , \quad k = ch, n, P \qquad (19)$$

The neutron and proton mean square radii are given by [24]:

$$\langle r^2 \rangle_k = \frac{4\pi}{k} \int_0^\infty dr \, r^4 \, \rho_k(r) \qquad (20)$$

The neutron skin thickness is a very important quantity utilized to describe the distributions of neutrons into nuclei. It is defined as the difference between the neutron and the proton *rms* radii as [22]:

$$t = \Delta r_{nP} = r_n - r_P = \langle rms \rangle_n^{1/2} - \langle rms \rangle_P^{1/2} \qquad (21)$$

The charge form factors are obtained from the ground-state CDD, where the form factor is simply transformed to the CDD with using the Fourier-Bessel transformations and vice versa [25, 26]. Therefore:

$$F_{ch}(q) = \frac{4\pi}{Z} \int_0^\infty \rho_{ch}(r) \, j_0(qr) \, r^2 \, dr \qquad (22)$$

where $j_0(qr) = \sin(qr)/qr$ is the zeroth order spherical Bessel function and q is the momentum transfer from the incident electron to the target nucleus. In the limit $q \to 0$, the target will be represented as a point particle, and the form factor of this target is equal to unity $F(q \to 0) = 1$.

Results and discussion

The ground-state properties of Ni-isotopes are studied with employing SHF method with ten types of Skyrme parameterizations listed in the Table 1. The investigated nuclear properties include charge, neutron, proton and mass densities with their associated radii, binding energies, neutron skin thickness and charge form factors.

Calculated charge rms radii are displayed in Table 2 and compared with the available experimental values [27]. Generally, it can be noticed that the increasing of the neutron number of the successive isotopes leads to a gradually increasing of the charge rms. There are excellent agreements between the calculated and

experimental values for ^{58}Ni, ^{60}Ni and ^{64}Ni isotopes with using SKM*, SKxs25 and SKxs20 parameterizations; respectively, while the calculated values for ^{61}Ni and ^{62}Ni with SLY4 set are close to the experimental ones as shown in Fig. 1. The calculated proton, neutron and mass radii are tabulated in Tables 3, 4, and 5, respectively. Inspection of these tables refers to a slight increasing of the calculated values for sequential isotopes, which attributed to the increasing of the neutron numbers. The proportional relation between the rms radius and the additional neutrons implies nuclear size extension, which attributed to the nuclear interaction between the supplementary neutrons and the other nucleons. Therefore, the calculated values of rms radii are found to be enlarging slightly from the isotope with low A up to that with high A.

Table 1: The Skyrme parameterizations used in the present work.

	t_0	t_1	t_2	t_3	W_0	x_0	x_1	x_2	x_3	α
SKM [12]	-2645.0	385.0	-120.0	15595.0	130.0	0.09	0.0	0.0	0.0	0.167
SKM* [12]	-2645.0	410.0	-135.0	15595.0	130.0	0.09	0.0	0.0	0.0	0.167
SI [2]	-1057.3	235.9	-100.0	14463.5	120.0	0.56	0.0	0.0	1.0	1.0
SIII [13]	-1128.75	395.0	-95.0	14000.0	120.0	0.45	0.0	0.0	1.0	1.0
SKO [14]	-2103.7	303.4	791.7	13553.0	118.0	-0.211	-2.81	-1.46	-0.43	0.25
SKE [15]	-1140.25	309.6	-122.2	11608.1	111.45	0.798	0.0	0.0	1.632	0.8
SLY4 [16]	-2488.91	486.8	-546.4	13777.0	123.0	0.834	-0.344	-1.0	1.354	0.167
SKxs15 [17]	-2883.29	291.6	-314.9	18239.6	161.4	0.476	-0.254	-0.611	0.592	0.167
SKxs20 [17]	-2885.24	302.7	-323.4	18237.5	162.7	0.137	-0.255	-0.607	0.054	0.167
SKxs25 [17]	-2887.81	315.5	-329.3	18299.8	163.9	-0.186	-0.248	-0.601	-0.409	0.167

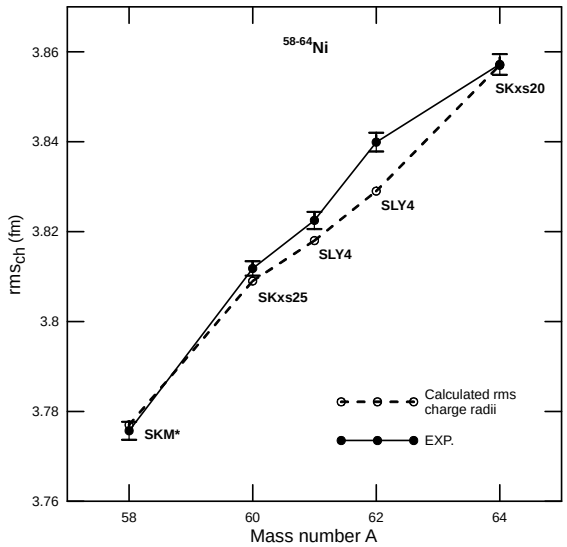

Fig. 1: Calculated rms charge radii for $^{58-64}$Ni isotopes compared with the experimental data taken from Ref. [27].

Table 2: Calculated charge rms radii (fm) using different Skyrme parameterizations in comparison with experimental data.

A	SKM	SKM*	SI	SIII	SKO	SKE	SLY4	SKxs15	SKxs20	SKxs25	Exp. [27]
58	3.755	3.777	3.699	3.815	3.752	3.720	3.791	3.793	3.797	3.804	3.7757±0.0020
60	3.771	3.793	3.722	3.837	3.765	3.743	3.807	3.804	3.805	3.809	3.8118±0.0016
61	3.783	3.805	3.737	3.851	3.776	3.756	3.818	3.815	3.815	3.817	3.8225±0.0019
62	3.794	3.816	3.752	3.865	3.786	3.769	3.829	3.826	3.824	3.825	3.8399±0.0021
64	3.826	3.847	3.783	3.893	3.818	3.798	3.859	3.859	3.857	3.856	3.8572±0.0023
66	3.858	3.879	3.814	3.921	3.851	3.826	3.888	3.892	3.889	3.887	--------

Table 3: Calculated proton rms radii (fm) for the selected Ni-isotopes.

A	SKM	SKM*	SI	SIII	SKO	SKE	SLY4	SKxs15	SKxs20	SKxs25
58	3.676	3.699	3.620	3.738	3.674	3.641	3.714	3.716	3.720	3.727
60	3.695	3.717	3.644	3.762	3.689	3.666	3.732	3.728	3.730	3.734
61	3.706	3.728	3.659	3.775	3.699	3.679	3.742	3.739	3.739	3.741
62	3.717	3.739	3.673	3.788	3.709	3.692	3.753	3.749	3.748	3.749
64	3.748	3.769	3.702	3.815	3.740	3.719	3.781	3.781	3.779	3.778
66	3.778	3.799	3.731	3.840	3.770	3.745	3.808	3.813	3.809	3.807

Table 4: Calculated neutron rms radii (fm) for the selected Ni-isotopes.

A	SKM	SKM*	SI	SIII	SKO	SKE	SLY4	SKxs15	SKxs20	SKxs25
58	3.673	3.693	3.611	3.730	3.686	3.624	3.713	3.700	3.710	3.722
60	3.737	3.756	3.669	3.793	3.756	3.675	3.776	3.757	3.772	3.789
61	3.779	3.798	3.700	3.823	3.801	3.710	3.814	3.794	3.812	3.831
62	3.820	3.838	3.730	3.852	3.845	3.742	3.850	3.830	3.851	3.873
64	3.887	3.905	3.787	3.907	3.913	3.795	3.911	3.893	3.917	3.941
66	3.948	3.966	3.839	3.958	3.977	3.845	3.966	3.952	3.978	4.006

Table 5: Calculated mass rms radii (fm) for the selected Ni-isotopes.

A	SKM	SKM*	SI	SIII	SKO	SKE	SLY4	SKxs15	SKxs20	SKxs25
58	3.674	3.696	3.615	3.734	3.680	3.632	3.713	3.707	3.715	3.724
60	3.717	3.738	3.657	3.778	3.725	3.671	3.756	3.743	3.752	3.763
61	3.746	3.766	3.681	3.801	3.755	3.696	3.781	3.769	3.778	3.790
62	3.774	3.794	3.704	3.823	3.785	3.720	3.806	3.794	3.805	3.817
64	3.827	3.846	3.750	3.867	3.838	3.762	3.855	3.845	3.857	3.870
66	3.877	3.896	3.794	3.908	3.890	3.803	3.900	3.893	3.908	3.923

The CDD are calculated according to SHF model and depicted in Figs. 2(a) – 2(f). The calculated CDD with SKM* parameterization that denoted by the blue curves are very close to the experimental data for the most regions of *r*. The inset figures are putted to present more explanations about the agreement between the calculated CDD with SKM* and experimental data. Unfortunately; there are no available experimental data for ^{66}Ni to compare with, but we can guess that the calculations with SKM* provide a good representation of the CDD as in the other nuclei.

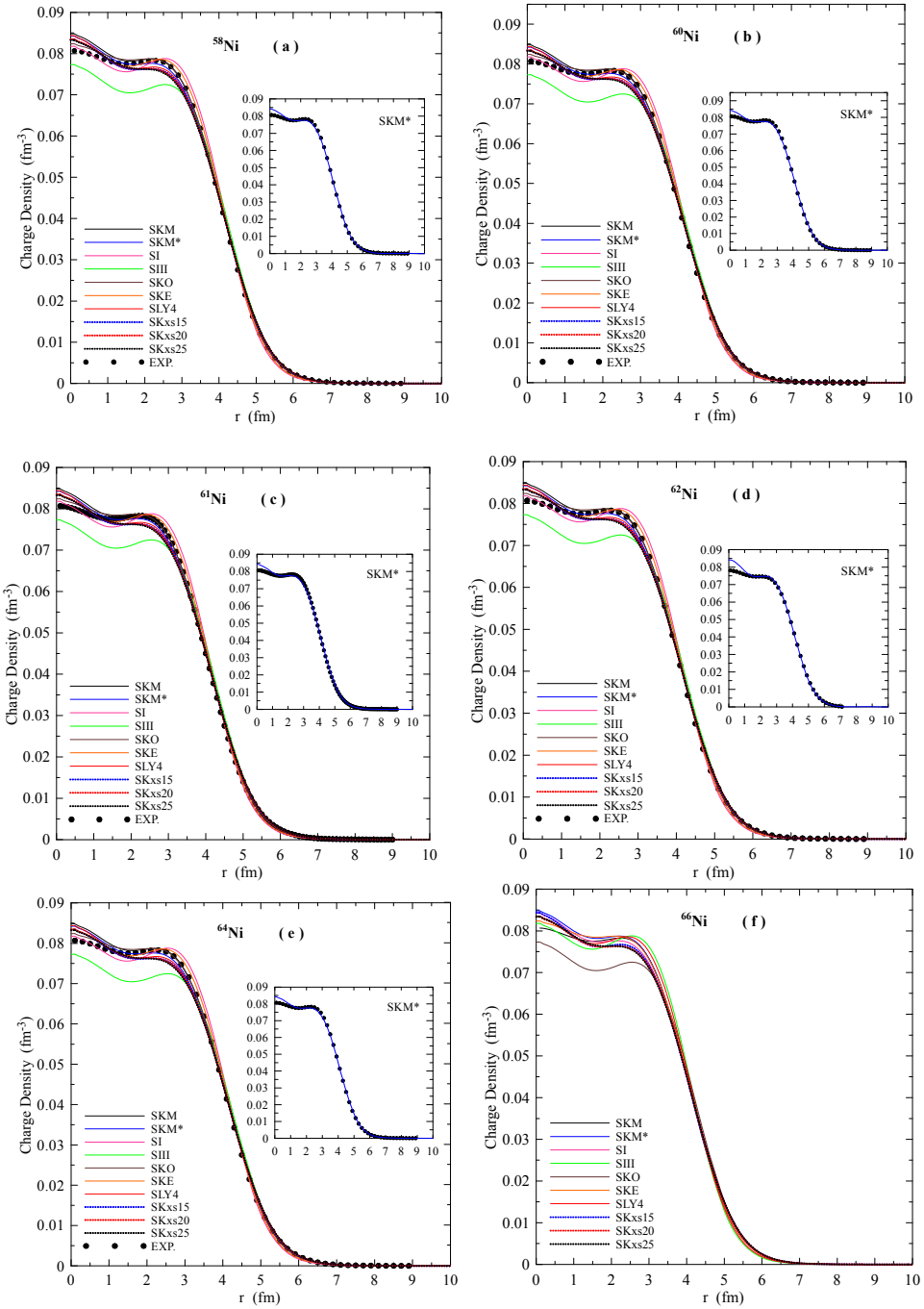

Fig. 2: Calculated charge density distributions for $^{58-64}$Ni isotopes. The inset figures are embedded to show the agreement between the calculated CDD with SKM* parameterizations and experimental data. The experimental data are taken from Ref. [28].

Since the SKM* parameterization is proved as a successful set to describe the CDD, this set is applied to calculate the proton, neutron and mass density distributions. The obtained results are plotted in Figs. 3(a) – 3(d) for all the considered nuclei. Figs. 3(a) and 3(b) show the behavior of the charge and the proton density distributions when the neutron numbers are increased. These distributions are depressed gradually in the succeeding isotopes, especially at the central regions and at the tail regions that illustrated by the inset figures. Figs. 3(c) and 3(d) present the density distributions of neutrons and nuclear mass. One can see from these figures the extensions of the neutron and the mass density distributions with adding neutrons to ^{58}Ni nucleus up to ^{66}Ni nucleus. These extensions that are noticed clearly at the fall-off and the surface regions, explained as a redistribution of nucleons due to the interaction with addition neutrons, where the nucleons are removed from the interior and from the tail regions and transferred into the farther regions.

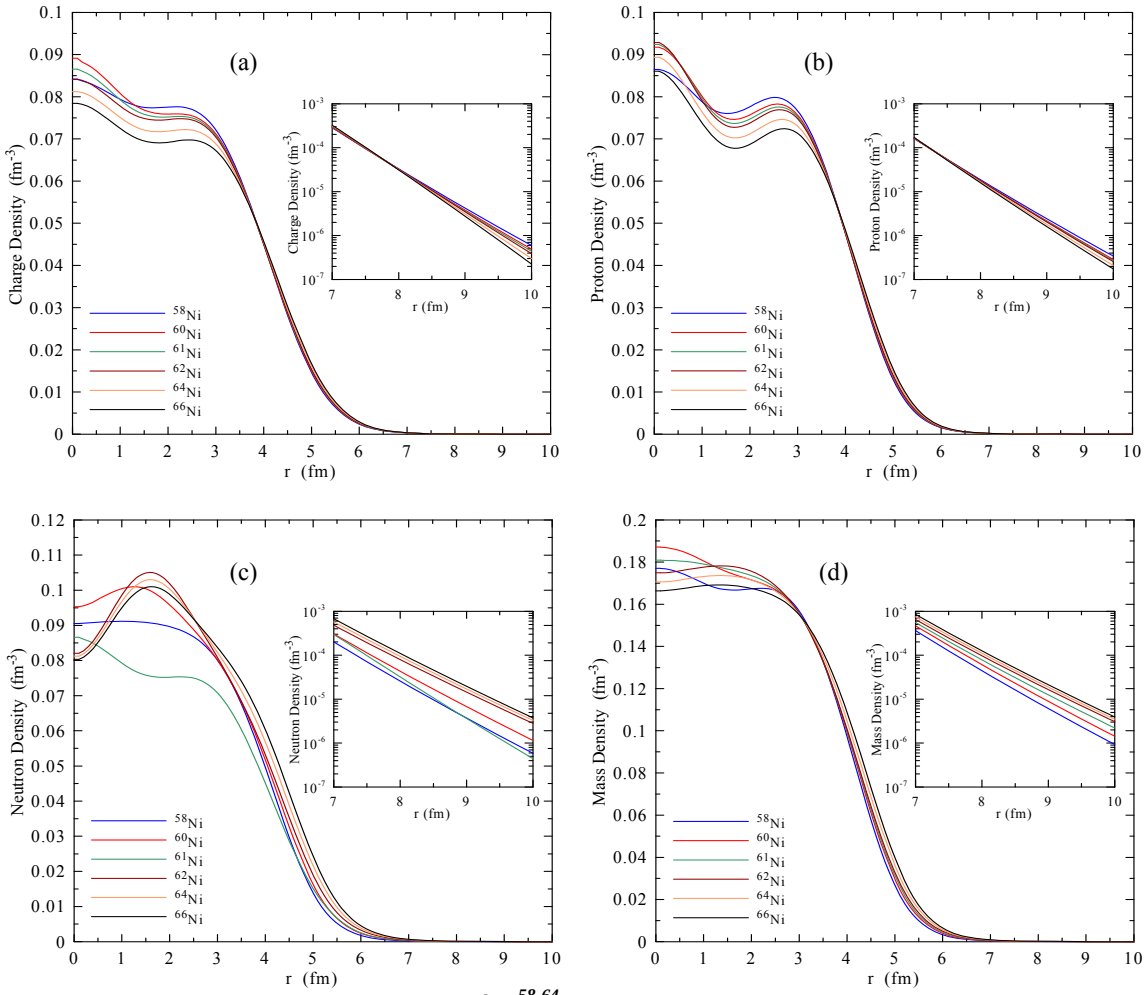

Fig. 3: Calculated density distributions for $^{58-64}$Ni isotopes using SKM* parameterization. The inset is in logarithmic scale. (a) charge density, (b) proton density, (c) neutron density and (c) mass density.

The total nuclear binding energies are calculated and listed in Table 6 together with the experimental results. The binding energies per nucleon are plotted in Fig.4 as a function of total nucleon number *A*. It can be noticed from Table 6 and Fig.4 that the calculated values of binding energies for ^{58}Ni, ^{60}Ni, ^{61}Ni, ^{62}Ni, ^{64}Ni and ^{66}Ni isotopes with using SLY4, SKxs15, SKxs20, SLY4, SKM* and SLY4 parameterizations, respectively, agree excellently with the corresponding experimental ones.

Table 6: The total binding energies (MeV) for the selected Ni-isotopes.

A	SKM	SKM*	SI	SIII	SKO	SKE	SLY4	SKxs15	SKxs20	SKxs25	Exp. [29]
58	518.793	508.864	531.421	504.659	511.415	510.982	506.360	504.773	504.081	503.344	506.458
60	540.262	530.569	550.439	523.775	532.083	531.335	528.047	526.998	526.323	525.617	526.845
61	548.201	538.655	558.035	532.123	539.834	538.821	536.482	535.644	534.981	534.304	534.665
62	556.103	546.684	565.669	540.551	547.429	546.185	544.967	544.084	543.424	542.780	545.261
64	571.032	561.656	581.045	557.653	563.265	561.939	560.699	560.241	559.740	559.303	561.757
66	586.463	577.118	596.556	575.075	579.324	577.736	577.062	576.414	576.058	575.810	576.807

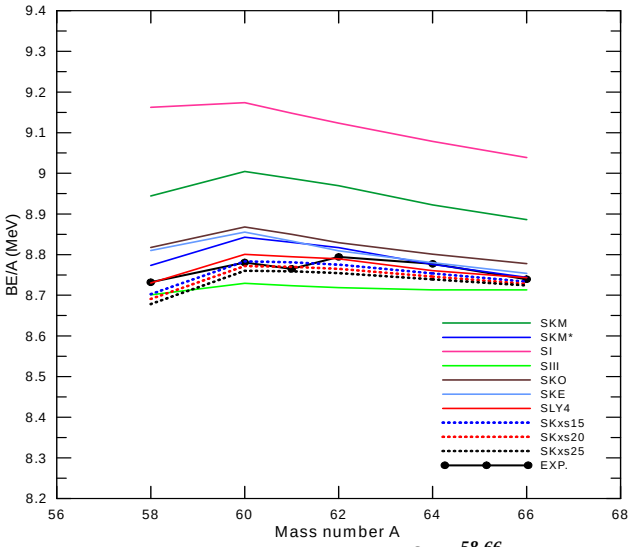

Fig.4: Calculated binding energies per nucleon for $^{58-66}$Ni isotopes compared with experimental data taken form Ref. [29].

The neutron skin thickness is defined as the difference between rms radii of neutrons and protons and represents the surplus of neutrons at the surface regions of nuclei. The neutron skin thickness is calculated for each considered isotope and presented in the Table 7 and plotted in Fig. 5. It can be noticed from the mentioned table and figure that the neutron skin thickness of Ni-isotopes increase progressively with increasing of neutron number. The negative values of ^{58}Ni isotope show that the proton rms radii are larger than the neutron rms radii.

Table 7: Calculated neutron skin thickness (fm) for the selected Ni-isotopes.

A	SKM	SKM*	SI	SIII	SKO	SKE	SLY4	SKxs15	SKxs20	SKxs25
58	-0.003	-0.006	-0.009	-0.008	0.013	-0.017	-0.001	-0.016	-0.010	-0.005
60	0.042	0.039	0.025	0.030	0.067	0.009	0.045	0.028	0.042	0.055
61	0.073	0.070	0.042	0.048	0.102	0.031	0.072	0.055	0.073	0.089
62	0.103	0.099	0.057	0.064	0.136	0.050	0.097	0.081	0.103	0.123
64	0.139	0.136	0.085	0.092	0.173	0.077	0.130	0.112	0.138	0.163
66	0.170	0.167	0.109	0.117	0.206	0.099	0.158	0.139	0.169	0.199

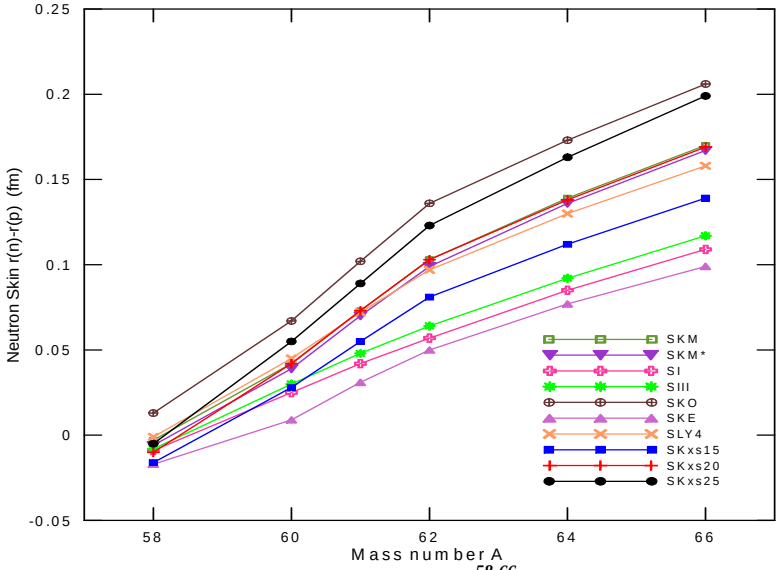

Fig. 5: The neutron skin thickness for $^{58-66}$Ni isotopes.

The charge form factors of the investigated isotopes are deduced in terms of the CDD that calculated with SKM* parameterization. The obtained results are presented in Fig.6 and compared with the experimental data that represented by the hollow circles. The calculated form factors are in excellent agreement with experimental data along all momentum transfer ranges as well as throughout the first and the second diffraction minima that located at $q \approx 1.05$ fm^{-1} and $q \approx 1.75$ fm^{-1}, respectively.

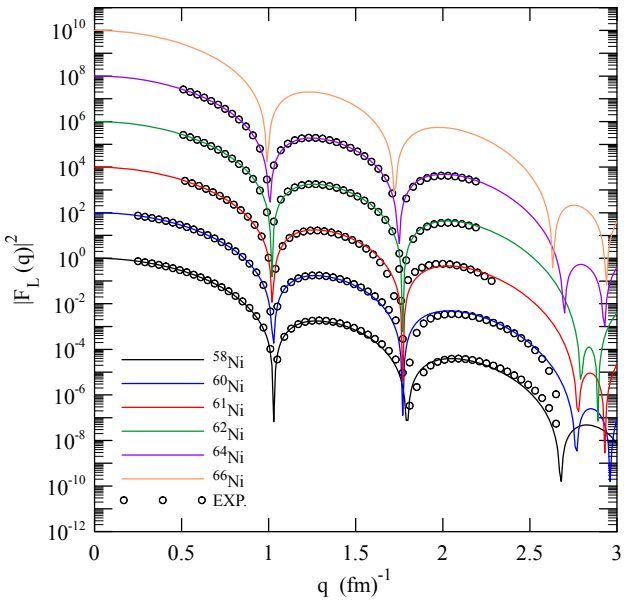

Fig. 6: The charge form factors calculated with SKM* parameterization for ^{58}Ni, ^{60}Ni (× 10^{2}), ^{61}Ni (× 10^{4}), ^{62}Ni (× 10^{6}), ^{64}Ni (× 10^{8}) and ^{66}Ni (× 10^{10}). The experimental data are taken from Ref. [28].

Conclusions

The ground-state properties of $^{58\text{-}66}$Ni isotopes are studied and calculated using the SHF method with several types of Skyrme parameterizations. The charge, neutron, proton and mass density distributions, the associated rms radii, the binding energies, the neutron skin thickness and the charge form factors are calculated and compared with the available experimental data. The obtained results lead us to outline the following conclusions:

1. The calculated charge rms radii are found to be larger than the calculated proton rms radii for all investigated isotopes.
2. The calculated charge rms radii for ^{58}Ni, ^{60}Ni, ^{61}Ni, ^{62}Ni and ^{64}Ni isotopes with using SKM*, SKxs25, SLY4, SLY4 and SKxs20 parameterizations, respectively, are in excellent agreement with the experimental results.
3. The obtained CDD curves using SKM* set show the best agreement with the experimental data in comparison with these curves that deduced using the other Skyrme sets.
4. The calculated binding energies for ^{58}Ni, ^{60}Ni, ^{61}Ni, ^{62}Ni, ^{64}Ni and ^{66}Ni isotopes using SLY4, SKxs15, SKxs20, SLY4, SKM* and SLY4 parameterizations, respectively, are in close agreement with the experimental values.
5. The charge form factors deduced using SKM* set are remarkably coincide with the experimental data.

References

[1] T. H. R. Skyrme, Nucl. Phys., 9 (1959) 615-634.

[2] D. Vautherin and D. M. Brink, Phys. Rev., C5 (1972) 626-674.

[3] C. B. Dover and N. V. Giai, Nucl Phys., A190 (1972) 373-400.

[4] K. W. Schmid and P. G. Reinhart, Nucl. Phys., A530 (1991) 283-302.

[5] H. Aytekin, Mod. Phys. Lett., A26 (2011) 1413-1425.

[6] E. Tel, H. M. Sahin, A. Kaplan, A. Aydin, T. Altinok, Ann. Nucl. Energy, 35 (2008) 220-227.

[7] E. Tel, R. Baldik, H. Aytekin, A. Aydin, Ann. Nucl. Energy, 36 (2009) 1333-1339.
[8] H. Aytekin, R. Baldik, E. Tel, Phys. Atomic Energy, 73 (2010) 922-926.
[9] A. A. Alzubadi, Z. A. Dakhil, T. Sheimaa, J. Nucl. Particle Phys., 7 (2014) 155-163.
[10] A. A. Alzubadi, Indian J. Phys., 89 (2015) 619-627.
[11] Y. Yulianto and Z. Su'ud, J. of Phys., Conf. Series, 799 (2017) 1-5.
[12] J. Bartel, P. Quentin, M. Brack, C. Guet, H. B. Hakansson, Nucl. Phys., A386 (1982) 79-100.
[13] M. Beiner, H. Flocard, N. V. Giai, P. Quentin, Nucl. Phys., A238 (1975) 29-69.
[14] P. G. Reinhard, D. J. Dean, W. Nazarewicz, J. Dobaczewski, J. A. Maruhan, M. R. Strayer, Phys. Rev., C60 (1999) 014316.
[15] J. Friedrich and P. G. Reinhard, Phys. Rev., C33 (1986) 335-351.
[16] E. Chabanat, P. Bonche, P. Haensel, J. Meyer, R. Schaeffer, Nucl. Phys., A635 (1998) 231-256.
[17] B. A. Brown, G. Shen, G. C. Hillhouse, G. Meng, A. Trzcinska, Phys. Rev., C76 (2007) 034305.
[18] W. Greiner and J. Maruhn: Nuclear Models, Springer-Verlag, Berlin, (1996) 2nd Ed.
[19] H. Aytekin, R. Baldik, H. Alici, Ann. Nucl. Energy, 46 (2012) 128-133.
[20] T. Lesinski, M. Bender, T. Duguet, J. Meyer, Phys. Rev., C76 (2007) 014312.
[21] J. Erler, P. Klupfel, P. G. Reinhard, J. Phys. G, Nuclear and Particle Physics, 38 (2011) 1-43.
[22] M. Brack, C. Guet, H. B. Hakansson, Phys. Rep., 123 (1985) 275-364.
[23] E. B. Suckling, "Nuclear Structure and Dynamics from the Fully Unrestricted Skyrme-Hartree-Fock Mod" Ph.D. Thesis, University of Surrey, (2011).
[24] A. Al-Rahmani, Ind. J. Phys., 90 (2016) 461-467.
[25] H. Uberall, "Electron scattering from complex nuclei part B", Academic Press, New York, (1971).
[26] T. deForest and J. D. Walecka, Adv. Nucl. Phys., 15 (1966) 1-109.
[27] I. Angeli and K. P. Marinova, At. Data Nucl. Data Tables, 99 (2013) 69-95.
[28] H. De Vries, C. W. De Jager, C. De Vries, At. Data. Nucl. Data Tables, 36 (1987) 495-536.
[29] M. Wang, G. Audi, A. H. Wapstra, F. G. Kondev, M. MacCormick, X. Xu, B. Pfeiffer, Chinese Phys., C36 (2012) 1603-2014.